

Anelastic behavior of 8Y-FSZ/Al₂O₃ composite

Rumi Kitazawa · Susumu Horibe · Tohru S. Suzuki

Received: 9 May 2008 / Accepted: 16 September 2008 / Published online: 9 October 2008
© Springer Science+Business Media, LLC 2008

Abstract This paper has clarified the anelasticity of 8Y-FSZ/ α -alumina composites wherein the 8Y-FSZ phases are dispersed like islands. The amount of anelastic strain generated and the manner of anelastic deformation were compared to those of monolithic 8Y-FSZ. The anelastic strains of six kinds of 8Y-FSZ/ α -alumina, as well as of monolithic 8Y-FSZ and monolithic α -alumina, were measured. The results showed that the anelastic strain was produced even in the composite where 8Y-FSZ phases existed as islands, and that the more the anelastic strain produced, the higher the volume fraction of 8Y-FSZ. In addition, the composition with a fully densified alumina phase had the effect of inhibiting anelastic strain in the 8Y-FSZ phase.

Introduction

Several years ago, Pan and Horibe [1] reported the anelastic behavior of Y₂O₃-doped ZrO₂ as a new toughening mechanism. This anelastic behavior is shown comprehensively in Fig. 1. When stress is applied abruptly to this material, strain is not induced simultaneously, but rather forms gradually in a time-dependent manner. Furthermore, after the load is removed, the non-elastic strain

produced is completely recoverable in a certain period of time (3,000–4,000 s) depending on the level of load and loading time. This recoverable strain, that is, anelastic strain, is supposed to release any concentration of stress that might lead to fatal damage in the brittle material. Anelastic strain tends to be saturated by holding a load for an extended amount of time [2]. Anelastic strain production increases as grain size increases, and the anelastic behavior is strongly affected by the testing temperature [3, 4]. A higher temperature enables the material to possess much more anelastic strain. The anelastic behavior depends on the kind of dopant [5], and it also depends strongly on the orientation of the crystal as well as the internal friction. From these results, Okada et al. [6] concluded that anelastic strain is produced mainly by a slight shift of ions along with the $\langle 111 \rangle$ cation–oxygen vacancy dipole.

Zirconia/alumina composite is receiving attention as a material for implants, structures, cutting tools, and so on, and 8Y-FSZ (8 mol% yttria fully stabilized zirconia)/alumina composite is also being studied with reference to many applications. Tekeli et al. [7] reported that doping alumina caused slower grain growth by researching the adding effect of 1 wt% α -alumina to high-purity 8 mol% yttria-stabilized cubic zirconia (c-ZrO₂). French et al. [8] investigated and compared the mechanical properties and fracture morphologies of seven different 8Y-FSZ/alumina composites: 8Y-FSZ volume fractions of 0, 0.05, 0.25, 0.5, 0.75, 0.95, and 1. They reported that Young's modulus, strength, toughness, and hardness of the composites decreased linearly with increases in the volume fraction of 8Y-FSZ and that the composites did not show R-curve behavior. The fracture morphology changed from intergranular fracture, for the tough alumina, to transgranular fracture, for the 8Y-FSZ, and the composites exhibited a mixed behavior of both fracture modes [8].

R. Kitazawa · S. Horibe (✉)
Department of Materials Science and Engineering, Waseda
University, 3-4-1, Ohkubo, Shinjuku-ku, Tokyo 169-8555, Japan
e-mail: horibe@waseda.jp

T. S. Suzuki
National Institute for Materials Science, 1-2-1, Sengen, Tsukuba,
Ibaraki 305-0047, Japan

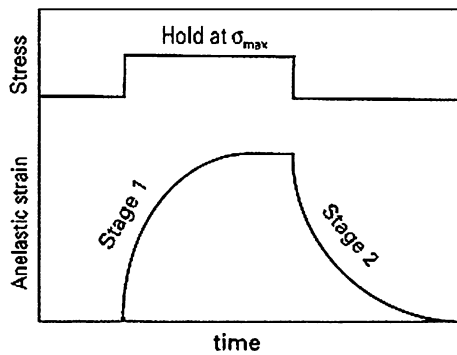


Fig. 1 Schematic illustration of anelastic behavior of yttria stabilized zirconia [1]

As mentioned above, 8Y-FSZ has been used in many composite materials, but no existing reports have focused on its anelasticity. Therefore, in this work, we have tried to discover whether the anelasticity of an 8Y-FSZ/ α -alumina composite is generated to the same degree as that of monolithic 8Y-FSZ, and whether it is produced in a similar manner even in the composite containing a lower volume fraction of 8Y-FSZ, wherein the 8Y-FSZ phases are dispersed like islands.

Experimental procedure

Specimen preparation

Commercial high-purity α -alumina (AKP-50, Sumitomo Chemical Co., Ltd.) and 8Y-FSZ (TZ-8Y, Tosoh Co., Ltd.) powders with average particle sizes of 0.2 μm and 70 nm, respectively, were used as starting materials in this study. These powders were dispersed in distilled water by adding a polyelectrolyte (poly (ammonium) carboxylate, A6114, Toagohsei Co., Ltd.) with the aid of ultrasounds. A deflocculated suspension with a 30 vol.% solid content, the composition of which was 70 vol.% 8Y-FSZ—30 vol.%

Al_2O_3 and 30 vol.% 8Y-FSZ—70 vol.% Al_2O_3 , was then prepared. The suspension was consolidated by slip casting and further densified by cold isostatic pressing at 392 MPa. The green compacts were sintered at 1,650 $^\circ\text{C}$ for 2 h or 7 h in air. To investigate the effect of porosity on the anelastic behavior in composite materials, 8Y-FSZ/ α - Al_2O_3 composites containing porous α - Al_2O_3 were also prepared. Monolithic 8Y-FSZ and monolithic α - Al_2O_3 were also used for comparison. The specimen designations are given in Table 1. Flexure bar test specimens with dimensions of 4.0 mm in depth, 3.5 mm in width, and 35 mm in length were machined from the sintered bodies. The specimens were polished with 0.25 μm Al_2O_3 abrasive paste to remove the microcracks from their surfaces.

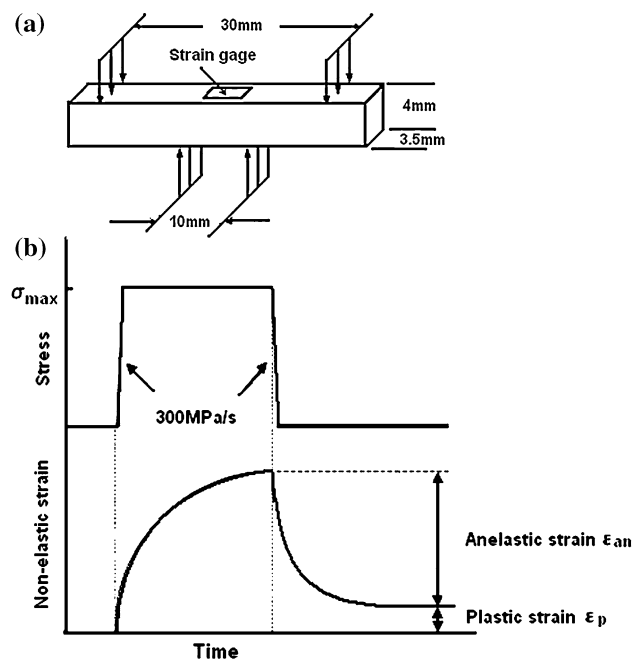


Fig. 2 Schematic explanation of **a** test piece and **b** the procedure of measurement of anelastic behavior (anelastic strain and plastic strain are defined as indicated)

Table 1 Designation, volume fraction, average grain size, and Young’s modulus of the composites

Composite	Volume fraction (vol.%)		Average grain size (μm)		Young’s modulus (GPa)
	8Y-FSZ	α -alumina	8Y-FSZ	α -alumina	
73S	70	30	1.24	0.66	257
73L	70	30	1.68	0.92	252
37S	30	70	0.74	1.06	324
37L	30	70	1.02	1.50	320
73P	70	30	–	–	112
37P	30	70	–	–	216
8Y	100	0	5.15	–	209
A	0	100	–	13.8	356

The microstructures of the sintered specimens were observed using a scanning electron microscope (SEM) for polished and thermally etched surfaces. The specimen surfaces were thermally etched at 1,450 °C for 1 h, and sputter deposited using Pt. The accelerating voltage of SEM was 10 kV, and secondary electrons were employed for observation. In the two-phase materials, the average grain size d_{avg} of each phase is calculated by the following equation:

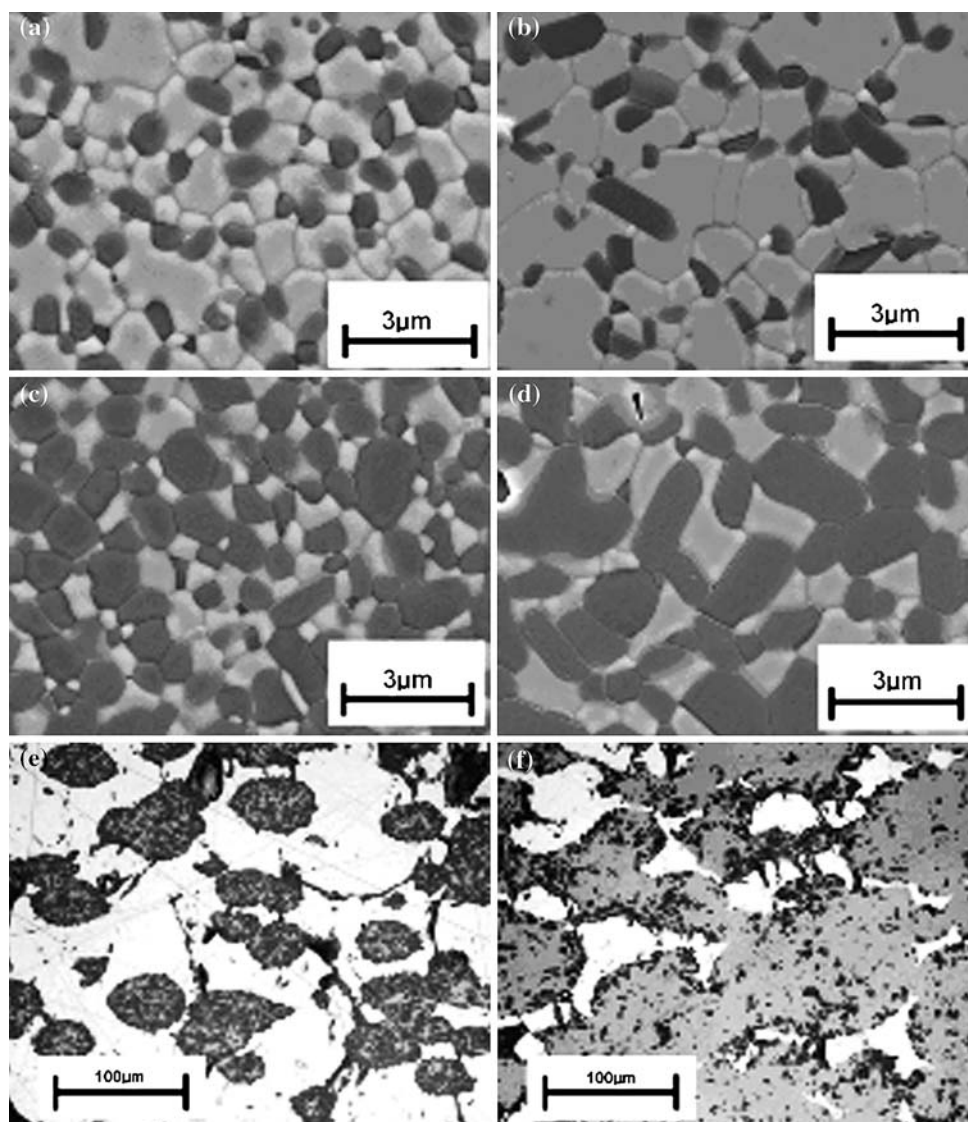
$$d_{\text{avg}} = 2c \sqrt{\frac{Af}{\pi n}} \quad (1)$$

where c is the constant for compensation which is used in a line-intercept method, 1.225 [9], A is the area of the SEM photograph, f is the volume fraction of the phase, and n is the number of grains observed in the SEM photograph.

Measurement of anelastic behavior

A strain gauge was attached to the center of the specimen surface, as shown in Fig. 2a. A four-point bending test was carried out at RT, with inner and outer spans of 10 and 30 mm, respectively. The desired load was applied abruptly to the specimen to avoid the generation of anelastic strain during the loading process. The applied load was maintained at the maximum stress level for 1 h, after which it was removed abruptly and the specimen was left for 1 h (Fig. 2b). The loading (unloading) speed was 300 MPa/s. The strain over time was measured using a strain gauge attached to the tensile surface of the specimen. The load and strain values were recorded as voltage signals using an oscillographic recorder, and non-elastic strain behavior was analyzed using a personal computer. Such high-quality digital analysis enabled us to investigate slight changes in

Fig. 3 Microstructures of polished specimens: **a** 73S, **b** 73L, **c** 37S, **d** 37L, **e** 73P, **f** 37P (white phases and gray phases are 8Y-FSZ and α -Al₂O₃, respectively, and dark dots in 73P and 37P are pores)



strain with great precision. The non-elastic strain, $\epsilon_{\text{non-elastic}}$, was calculated using the following equation:

$$\epsilon_{\text{non-elastic}} = \epsilon_{\text{total}} - \sigma/E \tag{2}$$

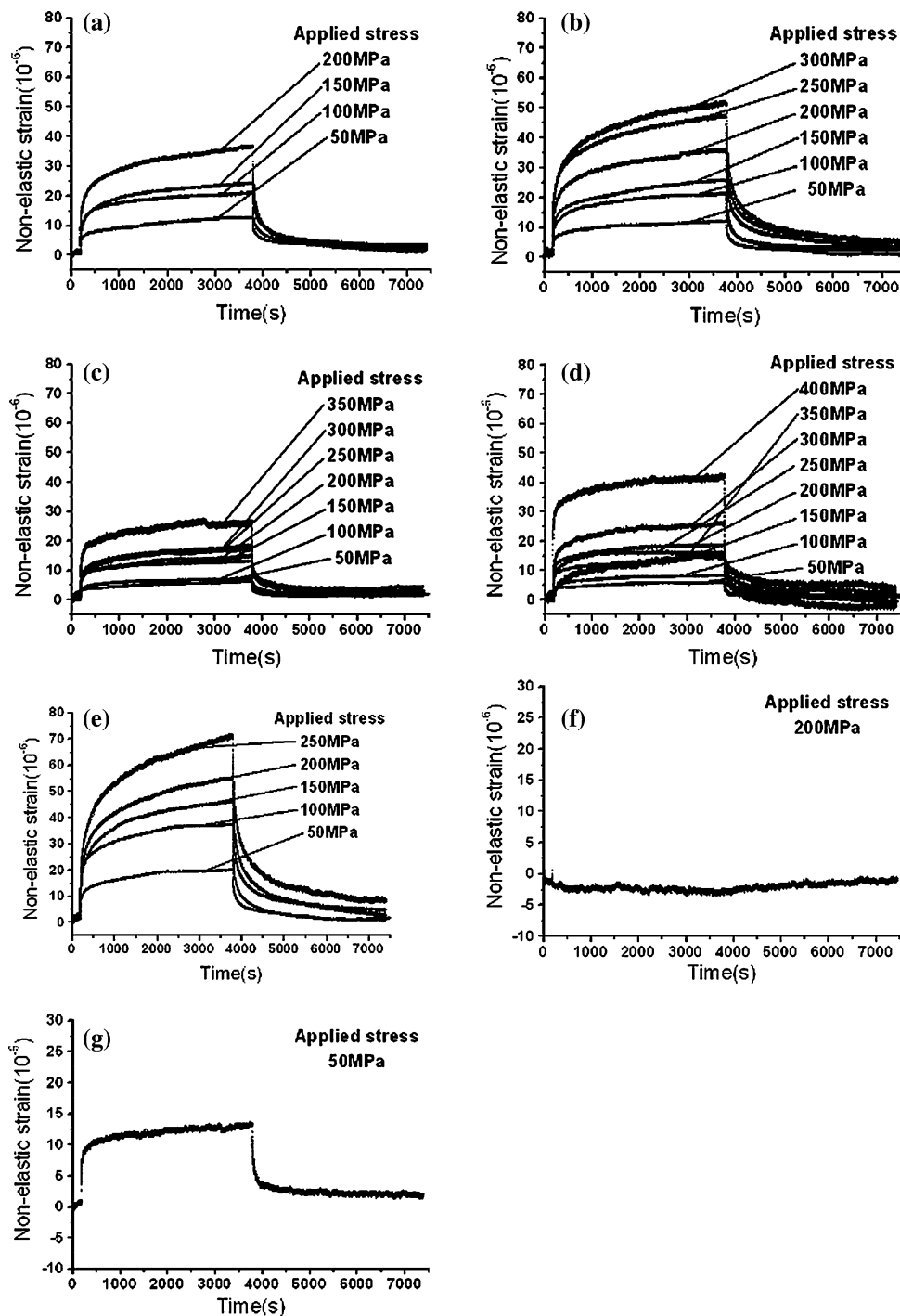
where ϵ_{total} is the total strain and σ is the stress. E is Young's modulus (shown in Table 1), which was calculated from the slope of the stress–strain loading curve in the stress range of about 10–30 MPa, supposedly the most suitable range excluding the influence of anelasticity. In the non-elastic

strain curve (Fig. 2b), the recoverable and non-recoverable strains after unloading were defined as the amounts of anelastic strain ϵ_{an} and plastic strain ϵ_{p} , respectively.

Results and discussion

Microstructures of the polished surfaces observed under the SEM are shown in Fig. 3. It is clear that 8Y-FSZ grains

Fig. 4 The experimental result of non-elastic behavior in seven materials: **a** 73S, **b** 73L, **c** 37S, **d** 37L, **e** 8Y, **f** A, **g** 37P



were almost isolated in 37S and 37L, although touching of 8Y-FSZ grains was partly observed in 37L. The average grain size of each phase, density, and Young's modulus of the composites are shown in Table 1.

Figure 4 shows the experimental result of non-elastic strain behavior in seven kinds of materials (73S, 37S, 73L, 37L, 8Y, 37P, and A) loaded every 50 MPa under the flexural condition (50 MPa → 100 MPa → 150 MPa → ...). The amounts of non-elastic strain produced in 73S, 37S, 73L, 37L, and 8Y increased with increase in the applied stress. In the composite materials and 8Y-FSZ, the non-elastic strain produced recovered almost fully after unloading. This indicates that the non-elastic strain was composed of anelastic strain ϵ_{an} without plastic strain ϵ_p . Non-elastic strain was not observed in alumina (A), even at 200 MPa. Figure 5 is the result for 73P, showing one series of non-elastic behavior at an identical stress of 50 MPa, where a loading–unloading sequence was repeated twice in succession. The ϵ_p detected only in this material decreased after the loading–unloading cycle, although the cumulative plastic strain $\epsilon_{c,p}$ increased. However, it should be noted that the ϵ_{an} values for each cycle were almost the same. This suggests that irreversible strain arose from decohesion or fracture in porous alumina due to stress loading and was saturated after several cycles.

Figure 6 shows the relationship between the ϵ_{an} value and the applied stress in the materials used. Anelastic strain ϵ_{an} was not detected in alumina (A). As stress increased, the ϵ_{an} values increased in 73S, 37S, 73L, 37L, and 8Y, with the following order: 37S \approx 37L < 73S \approx 73L < 8Y. The reason for the ϵ_{an} values of 73P and 37P being higher than those for the other composites with the same volume fractions of 8Y-FSZ will be discussed in the next paragraph. Figure 7 indicates the relationship between ϵ_{an} and the volume fraction of 8Y-FSZ. The prediction based on the linear rule of mixture roughly, but not completely, agrees with the experimental data, as shown in Fig. 7. This figure shows that the anelastic strain produced in the composite materials was slightly lower than the predicted strain.

It is significant that, in the case of composites, the stresses allocated to each phase (8Y-FSZ and α -Al₂O₃ in the present study) during the normal four-point bending test differed according to differences in Young's modulus and the coefficients of thermal expansion. The external stress applied to the 8Y-FSZ phase, σ_{8Y-FSZ} , was calculated from the following formula:

$$\sigma_{8Y-FSZ}/E_{8Y-FSZ} = \sigma_{composite}/E_{composite} \quad (3)$$

where $\sigma_{composite}$ is the stress applied to the whole specimen and E_{8Y-FSZ} and $E_{composites}$ are the Young's modulus of 8Y-FSZ(8Y) and the composite, respectively. As has been previously described, the ϵ_{an} values of 73P and 37P were higher than those of the other composites in spite of their containing the same volume fraction of 8Y-FSZ. The

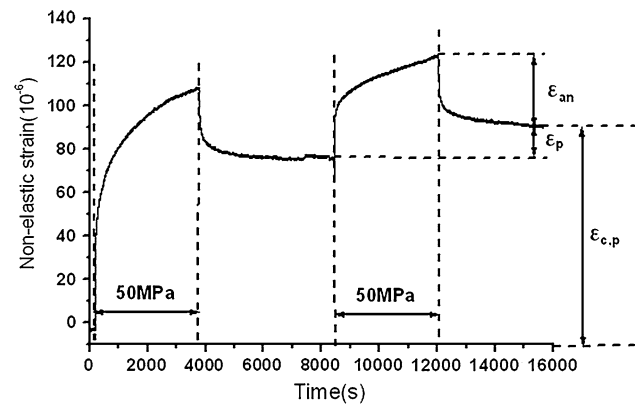


Fig. 5 One series of non-elastic behavior of 73P at a stress of 50 MPa

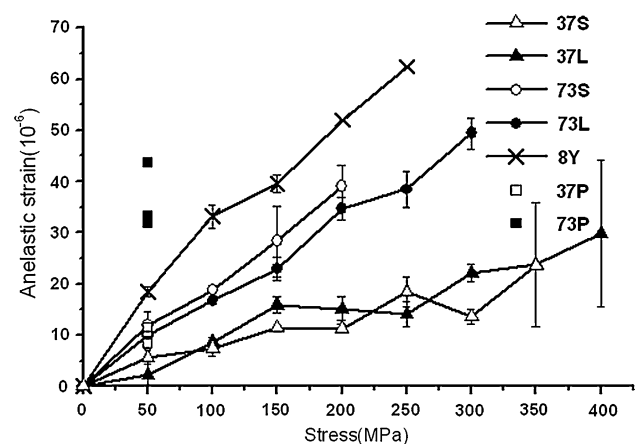


Fig. 6 The relationship between the ϵ_{an} value and the applied stress

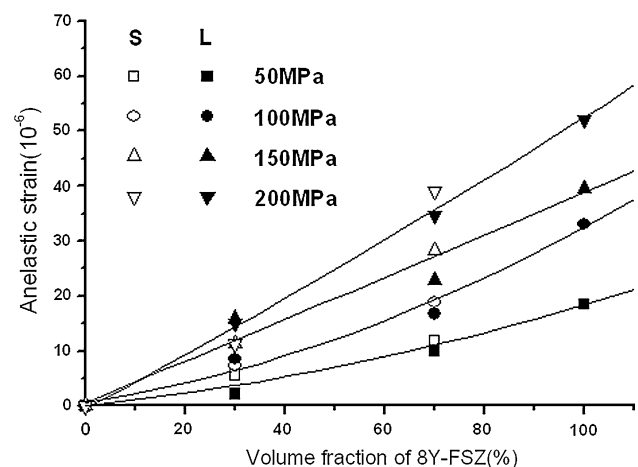


Fig. 7 The relationship between the ϵ_{an} value and the volume fraction of 8Y-FSZ

Young's modulus ($E_{composites}$) values for 73P and 37P are particularly low because of high porosity in the alumina phase. Therefore, the higher values of ϵ_{an} were concluded to be caused by the higher σ_{8Y-FSZ} along with the lower

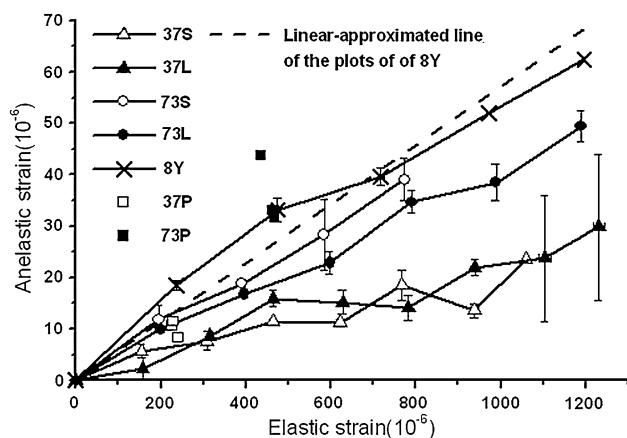


Fig. 8 The value of ε_{an} as a function of elastic strain

$E_{composites}$. The relationship between anelastic and elastic strain is shown in Fig. 8. The relative ε_{an} values were $37S \approx 37L < 73S \approx 73L < 8Y$. This is evidence that the composition of fully densified alumina inhibits the production of ε_{an} in the 8Y-FSZ phase with increase in the volume fraction of alumina, which amounts to anelasticity suppression of approximately 30% for 73S and 73L, and 70% for 37S and 37L. It is likely, therefore, that a composite consisting of porous alumina would be able to produce anelasticity expectedly. However, it should be noted that the strength of such porous materials is considerably lower.

Conclusion

Based on our research on the anelastic behavior of 8Y-FSZ/ α -Al₂O₃ composites, we conclude that:

- (1) Anelastic strain is produced even in composites wherein 8Y-FSZ phases exist as islands.

- (2) In the case of 8Y-FSZ/ α -Al₂O₃, which has a fully densified alumina phase, the more the anelastic strain produced, the higher the volume fraction of 8Y-FSZ. A composition with a fully densified alumina phase has the effect of inhibiting anelastic strain in the 8Y-FSZ phase.
- (3) In the case of 8Y-FSZ/ α -Al₂O₃, which has a porous alumina phase, the more the anelastic strain produced, the higher the volume fraction of 8Y-FSZ, as well as densified materials. However, the anelastic strain values are higher than those of composites containing fully densified alumina phases. A composition with a porous alumina phase does not inhibit, but instead retains, anelastic strain.

Acknowledgements The authors wish to thank Prof. Y. Kagawa and Dr. T. Tomimatsu at The University of Tokyo and Dr. Y. Sakka at National Institute for Materials Science for their support in the preparation and characterization of the composites. This research was supported by Waseda University Grant for Special Research Project (2006B-142, 2008B-146).

References

1. Pan LS, Horibe S (1996) J Mater Sci 31:6523. doi:10.1007/BF00356258
2. Matsuzawa M, Horibe S (2003) Mater Sci Eng 346:75. doi:10.1016/S0921-5093(02)00534-8
3. Matsuzawa M, Abe M, Horibe S (2003) ISIJ Int 43(4):555. doi:10.2355/isijinternational.43.555
4. Pan LS, Imai M, Horibe S (1997) Mater Sci Eng A 230:155. doi:10.1016/S0921-5093(97)00027-0
5. Matsuzawa M, Fujimagari E, Horibe S (2001) Mater Sci Eng A 314:105. doi:10.1016/S0921-5093(00)01937-7
6. Okada Y, Matsuzawa M, Horibe S (2007) J Mater Sci 42:5551. doi:10.1007/s10853-006-1090-8
7. Tekeli S, Erdogan M, Aktas B (2004) Ceram Int 30:2203. doi:10.1016/j.ceramint.2004.01.004
8. French JD, Chan HM, Harmer MP, Miller GA (1992) J Am Ceram Soc 75:418. doi:10.1111/j.1151-2916.1992.tb08196.x
9. Bernard-Granger G, Guizard C, Addad A (2008) J Am Ceram Soc 91:1703. doi:10.1111/j.1551-2916.2008.02335.x